Design of strain-introduced MZI interleaver on $LiNbO_3$ substrate*

ZHENG Yan-lin(郑燕琳)**, **CHEN Kai-xin**(陈开鑫), **and XIE Lu-wen**(谢璐雯)

College of Communication and Information Engineering, University of Electronic Science and Techonolgy of China, Chengdu 611731, China

(Received 27 August 2012)

A strain-introduced Mach-Zehnder interferometer (MZI) interleaver on lithium niobate ($LiNbO_3$) is proposed. The structure of the strain-introduced waveguide is designed in detail, and is produced by depositing a SiO_2 film on the annealed proton-exchanged $LiNbO_3$ waveguide. Considering the sensitivities of the edge strain to the deposition temperature and the thickness of the SiO_2 film, an optimum design of 50 GHz interleaver on this structure is given through analyzing the effective index changes for E^x_{pq} mode by finite difference method (FDM). The length of the bending waveguide in this interleaver is just two thirds of that in the conventional interleaver due to the high refractive index difference.

Document code: A **Article ID:** 1673-1905(2013)01-0004-5

DOI 10.1007/s11801-013-2339-5

Interleavers have been widely used in dense wavelength division multiplexed (DWDM) optical fiber communication system, because they allow existing DWDM filters which operate at wide channel spacing and can be extended to the system designed with narrow channel spacing in the range of 50 GHz or even less[1]. Although all of the three technology platforms of micro-optic, all-fiber[2], planar lightwave circuits (PLC) can be used to implement an interleaver, the PLC-based interleavers offer the advantages of being more compact and rugged compared with the other two[3].

One popular type of PLC-based interleavers is Mach-Zehnder interferometer (MZI) interleaver[4-6]. In recent years, a lot of efforts have been made to improve their performance, and among them, tuning function has been considered very important, because with this function, the center frequency can be adjusted to match the international telecommunication union (ITU) grid, and the light waves from the two output ports can be switched with each other. Both thermo-optic effect[7] and electro-optic effect can be utilized to realize the tuning function, and each has its own merits. However, compared with thermo-optic tuning, electro-optic tuning is with faster tuning speed, higher tuning accuracy and no heating interference[8]. Therefore, it is very promising to realize electro-optic tuning interleaver. Lithium niobate ($LiNbO_3$), which possesses excellent electro-optic, acousto-optic, piezoelectric and stable chemical performance, is an optimal material to fabricate aforementioned electro-optic tuning interleaver. However, because of small refractive index difference of the usual $LiNbO_3$ waveguide fabricated by proton exchange or Ti-diffusion, conventional structure of $LiNbO_3$ MZI interleaver, which is composed of two directional couplers and a pair of unbalanced curved arms with large radius, will be impossibly long. So fabricating such an interleaver is very difficult.

In this paper, we propose the strain-induced method to further increase the index contrast of annealed proton-exchanged $LiNbO_3$ waveguide so as to fabricate an electro-optic tuning interleaver with suitable size. Although there are some other ways to increase the index contrast, such as wet-etching diffusion technology[7], stain-introduced technology has the advantages of easy fabrication, low propagation loss and no change for the $LiNbO_3$ substrate composition. Strain-induced waveguides in various substrates, such as GaAS[9], lithium niobate, lithium tantaiate[10,11], and bulk sapphire substrates[12], have been demonstrated. And the strain is introduced selectively into the waveguide structure by the deposition of SiO_2 or SiN_y. In this paper, a layer of SiO_2 film is deposited on $LiNbO_3$ substrate by sputtering, and because of the large thermal mismatch between them, a large amount of strain is created when they cool down to room temperature. As a result, the largest localized refractive index change in the order of 10^{-3} is introduced via the elasto-optical effect.

* This work has been supported by the National Natural Science Foundation of China (No.61177054).

** E-mail: 491839926@qq.com

The conventional structure of $LiNbO_3$ MZI interleaver is shown in Fig.1(a). It consists of two 3 dB directional couplers connected by two asymmetric channel waveguide arms. One of the waveguides is straight, and the other is bending. Due to interference of the signals from the two waveguides, this interleaver can separate a comb of optical signal frequencies with a spacing of Δf, which may be split into two combs, both having the double-frequency-spacing[13] as

$$\Delta f = \frac{c}{2(n_{\text{eff}\,2}L - n_{\text{eff}\,2}\Delta L - n_{\text{eff}\,1}L)}\ , \tag{1}$$

where ΔL is the length difference between the two waveguide arms, n_{eff1} and n_{eff2} are the effective refractive indices of the straight waveguide and bending waveguide, respectively, and L is defined as the length of the straight guide or the length of the bending guide in horizontal direction. And in a conventional MZI interleaver, n_{eff1} is equal to n_{eff2}.

Fig.1(b) shows the specific structure of the two arms, where h is defined as the branch height. And the difference ΔL is given by:

$$\Delta L = 2\int_0^{L/2}\sqrt{1+\frac{4\pi^2 h^2}{L^2}\sin^2(\frac{2\pi x}{L})}\,\mathrm{d}x - L\ . \tag{2}$$

When ignoring model radiation loss, the total bending loss can be obtained by[14]:

$$\alpha(\mathrm{dB}) = \frac{10}{\ln 10}\frac{C_1 L}{\pi}\int_0^{\frac{\pi}{2}}\exp[-C_2 L^2\sec(x)/8\pi h]\,\mathrm{d}x\ , \tag{3}$$

where C_1 and C_2 are determined by the waveguide dimension (waveguide width W) and material parameters (refractive index of the substrate n_s and maximum refractive index difference Δn between the substrate and the surface) of the bending waveguide. Due to different exchanged and annealed time, the effective index and maximum refractive index difference on the surface are various. Here we consider the condition of Δn=0.015, and the other parameters are Δf=50 GHz, λ=1550 nm, W=6 μm, n_s=2.1381 and a=0.1 dB (isolation of about -25 dB). Combining Eqs.(1)-(3), we can calculate that the length L is 2.66 cm at least when the bending loss is not larger than 0.1 dB. Considering the lengths of the two couplers, the conventional MZI interleaver may be longer than 5.6 cm. Obviously, this size of device is too large to fabricate. To solve this problem, strain is introduced to the bending waveguide by depositing a layer of SiO_2 to increase the refractive index difference in $LiNbO_3$ substrate.

The proposed electro-optic tuning MZI interleaver can be fabricated as following steps. First, optical waveguide circuits which comprise a complete MZI interleaver are fabricated on $LiNbO_3$ substrate by annealed photon exchange method. Then for increasing refractive index difference and keeping

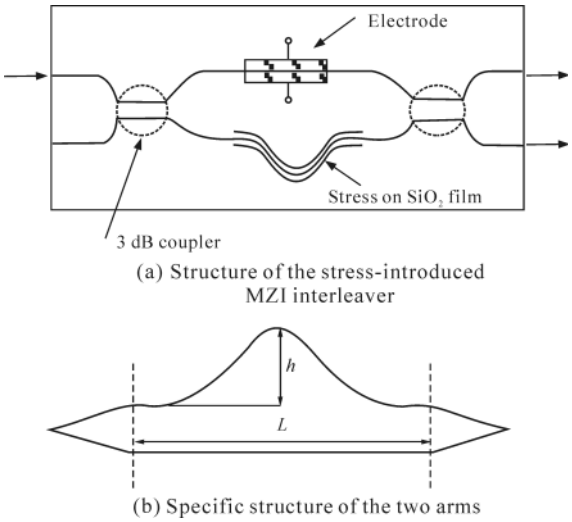

Fig.1 Configuration of the proposed electro-optic tuning MZI interleaver on $LiNbO_3$ substrate

a single a mode propagating in the bending waveguide, a layer of SiO_2 film with thickness of t is deposited on the substrate at high temperature T_d, and then cooled to room temperature T_r (20 °C). It introduces a compressive stress in the film, because the thermal expansion coefficient of the film α_f is less than that of the substrate α_s. At last, the sample is patterned again by standard photolithograph, and the SiO_2 film above the curved waveguide arm is removed by reactive ion etching. When a window is opened in the SiO_2 film, the edge of the window exerts a force on the $LiNbO_3$ substrate, and it is parallel to the surface of $LiNbO_3$ and perpendicular to the edge of the window. The force acts in a direction away from the window edge as shown in Fig.2. It produces a complex strain field in the substrate, which builds very high stress values immediately beneath the edge of SiO_2.

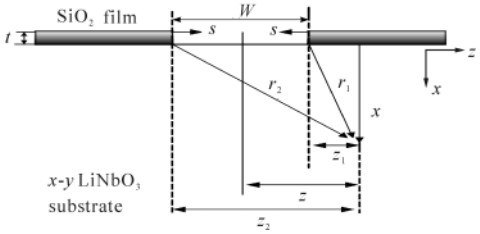

Fig.2 Configuration of stripe window for stress calculation

This edge force S (dyn/cm) determined by the thickness t of film and the average compressive stress σ_s in the film can be obtained as:

$$S = \sigma_s t\ . \tag{4}$$

The thickness t of film depends on the deposition temperature. Here, we calculate stress σ_s by ANSYS 12.0 finite element program, and the parameters of the SiO_2 and $LiNbO_3$ used in this model are given in Tab.1. From Fig.3(a), we know

that when the SiO_2 film with thickness of 1 μm is deposited on the $LiNbO_3$ substrate with thickness of 500 μm, the edge force is produced from -1.56 × 10^5 dyn/cm to -4.34 × 10^5 dyn/cm as the temperature increases from 300 °C to 800 °C.

Tab.1 Mechanical parameters used in strain calculation of Young's modulus (*E*), Possion's ratio (*v*) and thermal expansion coefficient (*α*) for SiO_2 and $LiNbO_3$[15]

	E (Pa)	*v*	*α* (m/K)
SiO_2	7.26×10^{10}	0.25	5.1×10^{-7}
$LiNbO_3$	1.70×10^{11}	0.164	4.1×10^{-6} ($\alpha^{//}$)
			14.8×10^{-6} ($\alpha^{\perp}$)

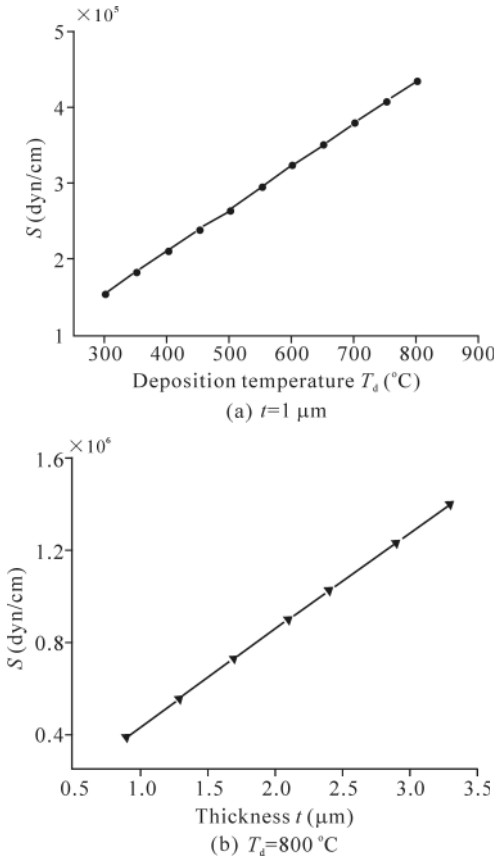

Fig.3 Edge force *S* calculated from ANSYS vs. deposition temperature T_d and thickness of SiO_2 film *t*

The applied force *S* causes the coordinates of point *P* to change from (*x*, *z*) to (*x* + *w*, *z* + *u*), and because of the symmetry of the configuration, there is no displacement in *y* direction. Kirkby and Selway[16] have given the displacement *u* in the *z* direction and the displacement *w* in the *x* direction as:

$$u = 2S\left[(AB-C)\ln(\frac{r_1}{r_2}) + A(\frac{z_1^2}{r_1^2}-\frac{z_2^2}{r_2^2})\right], \quad (5)$$

$$w = 2S\left\{A\left(\frac{z_1 x}{r_1^2}-\frac{z_2 x}{r_2^2}\right)+C\left[\cos^{-1}\left(\frac{x}{r_1}\right)-\cos^{-1}\left(\frac{x}{r_2}\right)\right]\right\}, \quad (6)$$

where x_1, x_2, r_1 and r_2 are defined in Fig.2. $A = (1 + v)/2\pi E$, B=3−4v, and $C = (1+v)(1-2v)/2\pi E$. The values of A, B and C depend on the Young's modulus E and Poisson's ratio v of the substrate, which are given in Tab.1.

Due to these displacements, we can calculate the non-zero elastic strain in the substrate as:

$$s_{zz} = \frac{\partial u}{\partial z} = 2S[A(\frac{z_1(r_1^2-2x^2)}{r_1^4}-\frac{z_2(r_2^2-2x^2)}{r_2^4})-C(\frac{z_1}{r_2^2}-\frac{z_2}{r_1^2})], \quad (7)$$

$$s_{xx} = \frac{\partial w}{\partial x} = 2S[(AB-C)(\frac{z_2^2}{r_2^2}-\frac{z_1^2}{r_1^2})-2Az^2(\frac{z_2}{r_2^4}-\frac{z_1}{r_1^4})]. \quad (8)$$

Fig.4(a) and (b) show the strain distributions in the horizontal direction (*z*) and the vertical direction (*x*) calculated for a 1 μm-thick SiO_2 film deposited at the temperature of 800 °C on the $LiNbO_3$ substrate with a 6 μm-wide stripe window. The contour lines are in units of strain of 10^{-4}, *T* is tension, and *C* is compression. The strains increase rapidly when the edge of the window is approached, and the contour lines crowd very closely together. Although in theory the two peak strain values (s_{zz}, s_{xx}) are infinite at the surface of the substrate under the edge of the window, we consider them as -4.92 × 10^{-2} and 1.6 × 10^{-2}, respectively, due to the finite thickness of the film and the plastic deformation. Because of the same width of the windows, the shape of the strains does not change obviously when increasing the deposition temperature or the thickness of the SiO_2 film.

Taking the elasto-optical effect in $LiNbO_3$ introduced by

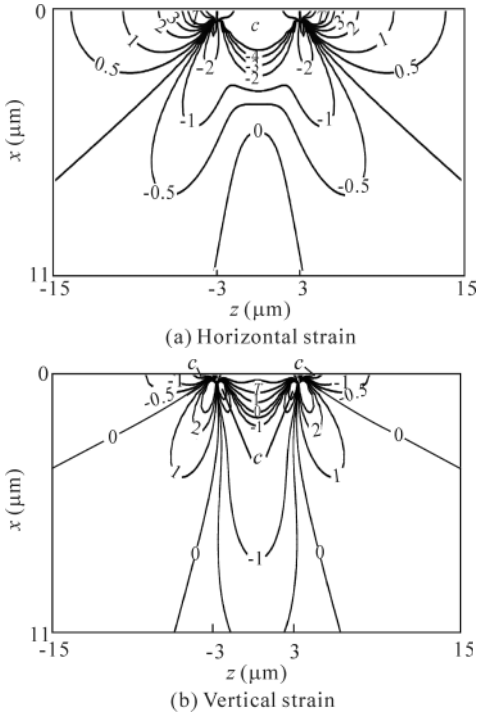

Fig.4 Strain distributions beneath the 6 μm-wide window

these strains into account, the change in the refractive index is determined for E_{pq}^{x} or E_{pq}^{y} model. The results for E_{pq}^{x} model are expressed as

$$\Delta n_{yy}(x,z) = -\frac{1}{2} n_y^3 [p_{12} s_{xx}(x,z) + p_{13} s_{zz}(x,z)] \quad , \tag{9}$$

$$\Delta n_{zz}(x,z) = -\frac{1}{2} n_z^3 [p_{31} s_{xx}(x,z) + p_{33} s_{zz}(x,z)] \quad , \tag{10}$$

where p_{ij} is the relevant photo-elastic tensor[17] of $LiNbO_3$, and n_y, n_z are the refractive indices of the annealed photon-exchanged $LiNbO_3$ substrate in the two directions, respectively. Fig.5 shows the refractive index change corresponding to the strains shown in Fig.4. In the calculation, we use the following values as p_{12}= 0.090, p_{13}=0.133, p_{31}=0.179, p_{33}= 0.071, n_y=2.2112 and n_z=2.21381 at λ=1550 nm. The index change in z direction shows a peak of 2.545 × 10^{-3} near the edges, and is 0.545 × 10^{-4} at the surface of the substrate in the window region. And with the increase of depth, the refractive index change decreases in the substrate, so the refractive index difference of the waveguide arms can be increased.

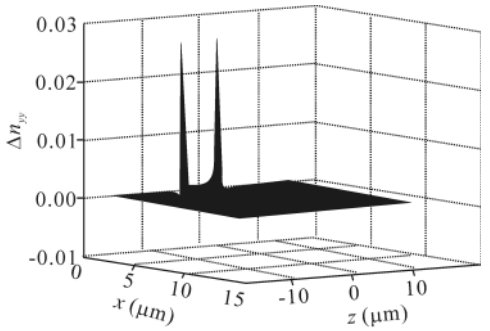

(a) Refractive change in y direction

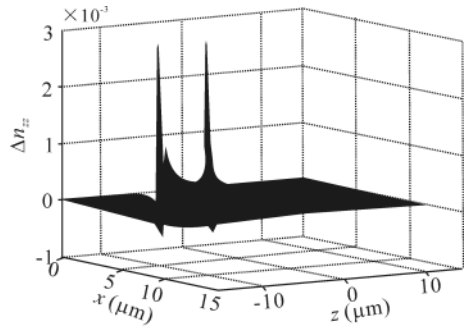

(b) Refractive change in z direction

Fig.5 Refractive index change profiles calculated from the strain in Fig.4

The induced strains make the refractive index in every point in $LiNbO_3$ changed, and to specifically analyze the influence of them, semivectorial polarized finite method[18] is used to calculate the effective index of the strain-introduced waveguide. The semi-vector wave function deduced from the wave function for E_{pq}^{x} mode can be obtained as

$$\frac{\partial}{\partial z}\left(\frac{\partial \varepsilon_z E_z}{\varepsilon_y \partial z}\right) + \frac{\partial E_z}{\partial x^2} + k_0^2(\varepsilon_z - n_{\text{eff}}^2)E_z = 0 \, , \tag{11}$$

where E_z is the electric field in z direction, k_0 is wavenumber, n_{eff} is effective index of the waveguide, and ε_i (i=x, y) is permittivity tenser. In this situation, they are equal to the sum square of the refractive index of annealed photon exchange substrate n_i and the strain-induced refractive index change Δn_{ii}. Applying finite difference calculations, Eq.(11) reduces to a five-node linear equation at every node in physical structure. Combining all the functions for all points, we obtain the following eigenvalue matrix equation:

$$\boldsymbol{AE} = k_0^2 n_{\text{eff}}^2 \boldsymbol{E} \, , \tag{12}$$

where $k_0^2 n_{\text{eff}}^2$ is eigenvalue, and $\boldsymbol{E}$ is corresponding eigenvector which represents the electric field profile E_z. $\boldsymbol{A}$ is a sparse matrix with 5×m nonzero values, where m is the total number of nodes considered in the physical structure. Then we impose Dirichlet and Neumann boundary conditions on the nodes on the edge of the analysis window and combing Eq.(12), the effective index and electric field distribution can be obtained.

The strains in the substrate can change along with deposition temperature or the thickness of the SiO_2 film. To analyze the influence of them, the effective indices under different T_d and t are calculated, as illustrated in Fig.6. The refractive index distribution of the annealed photon-exchanged $LiNbO_3$ substrate is the same as that of the $LiNbO_3$ waveguide without stress which is shown above. From Fig.6, we can conclude that the effective index increases when the deposition temperature or the thickness of the film is increasing. Hence, if a 3.3 μm-thick SiO_2 film is deposited on the substrate at 800 °C, it can be calculated that the effective index n_{eff} is 2.1414, the length of the two arms L is 1.78 cm, and the branch height h is 1.6 mm compared with n_{eff}=2.1405, L=2.66 cm, h = 1.98 mm in traditional MZI interleaver shown above.

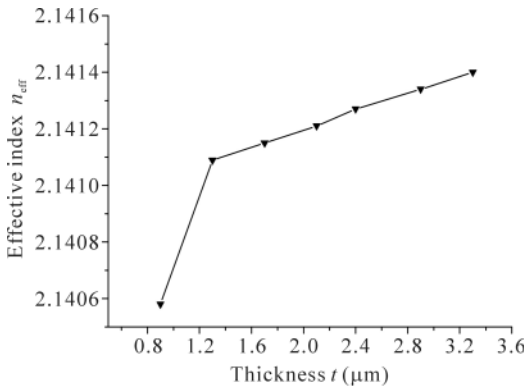

(a) T_d=800 °C

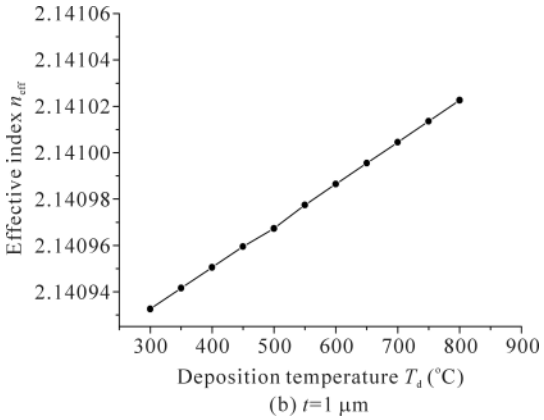

Fig.6 Effective index for E^x_{pq} mode vs. deposition temperature T_d and thickness of SiO_2 film t

In conclusion, a strain-introduced MZI interleaver on $LiNbO_3$ is proposed. Compared with the conventional MZI interleaver, this intreleaver is more compact without sacrificing any other performance. The whole length of it is not more than 4.7 cm, and also small channel spacing (50 GHz) and high isolation (-25 dB) can be obtained simultaneously.

References

[1] B. Shine and J. Bautista, J. Lightwave Technol. **8**, 140 (2000).

[2] ZHANG Bao-ge, TAO Cai-xia and LU Yan, Journal of Optoelectronics • Laser **21**, 1641 (2010). (in Chinese)

[3] H. P. Chan, Q. Wu, K. X. Chen, W. Y. Chan and B. P. Pal, International Photonics Global Conference (IPGC), Singapore, 2008.

[4] K. Jinguji and M. Oguma, J. Lightwave Technol. **18**, 252 (2000).

[5] Lian-Wee Luo, Salah Ibrahim, Arthur Nitkowski, Zhi Ding, Carl B. Poitras, S. J. Ben Yoo and Michal Lipson, Opt. Express **18**, 23079 (2010).

[6] K. X. Chen, H. P. Chan, F. S. Chen and W. Y. Chan, IEEE Photonics Technol. Lett. **23**, 1157 (2011).

[7] W. Tzyy-Jiann and C. Cha-Hong, IEEE Photonics Technol. Lett. **19**, 1904 (2007).

[8] W. Tzyy-Jiann, C. Cha-Hong and L. Che-Yung, Opt. Lett. **32**, 2777 (2007).

[9] M. Buda, G. Iordache, G. A. Acket, T. G. van der Roer, L. M. F. Kaufmann, B. H. van Roy, E. Smallbrugge, I. Moerman and C. Sys, IEEE J. Quantum Electron. **36**, 1174 (2000).

[10] O. Eknoyan, H. F. Taylor , Z . Tang, V. P. Swenson and J. M. Marx, Appl. Phys. **60,** 27 (1992).

[11] D. L. Tang, X. D. Zhang, G. H. Zhao, Z. Y. Dai, X. Lai and F. Guo, J. Zhejiang University-Science **10**, 595 (2009).

[12] M. Liu and H. K. Kim, Appl. Phys. **79**, 2693 (2001).

[13] R. M. de Ridder and C. G. H. Roeloffzen, Interleavers in Wavelength Filter for Fiber Optics, Springer Series in Optical Sciences, 381 (2006).

[14] J. M. William, K. K. Steven and C. A. Rod, IEEE J. Quantum Electron. **18,** 1802 (1982).

[15] W. J. Tropf, T. J. Harris and M. E. Thomas, Optical Materials: Visible and Infrared, in Electro-Optics Handbook, McGraw-Hill Press, 377 (2000).

[16] Kirkby P. A., Selway P. R. and Westbrook L. D., Appl. Phys. **50**, 4567 (1979).

[17] R. S. Weis and T. K. Gaylord, Appl. Phys. **37**, 191 (1985).

[18] E. Lea and B. L. Weiss, IEE Proc.-Optoelectron. **147**, 2 (2000).